ResearchGate

See discussions, stats, and author profiles for this publication at: https://www.researchgate.net/publication/361044058

Reconfigurable Fiber Wireless fronthaul with A-RoF and D-RoF co-existence through a Si3N4 ROADM for Heterogeneous mmWave 5G C-RANs

Article *in* Journal of Lightwave Technology · August 2022

DOI: 10.1109/JLT.2022.3179636

CITATIONS
0

READS
13

11 authors, including:

Eugenio Ruggeri
Aristotle University of Thessaloniki
23 PUBLICATIONS **144** CITATIONS

SEE PROFILE

Christos Vagionas
Aristotle University of Thessaloniki
135 PUBLICATIONS **956** CITATIONS

SEE PROFILE

Ronis Maximidis
Eindhoven University of Technology
28 PUBLICATIONS **56** CITATIONS

SEE PROFILE

George Kalfas
Aristotle University of Thessaloniki
76 PUBLICATIONS **631** CITATIONS

SEE PROFILE

Some of the authors of this publication are also working on these related projects:

chaotic synchronization View project

Ion Exchange Waveguides View project

All content following this page was uploaded by Christos Vagionas on 22 August 2022.

The user has requested enhancement of the downloaded file.

Reconfigurable Fiber Wireless fronthaul with A-RoF and D-RoF co-existence through a Si3N4 ROADM for Heterogeneous mmWave 5G C-RANs

Eugenio Ruggeri, Christos Vagionas, Ronis Maximidis, George Kalfas, Dimosthenis Spasopoulos, Nikos Terzenidis, Ruud M. Oldenbeuving, Paul W. L. van Dijk, Chris G.H. Roeloffzen, Nikos Pleros and Amalia Miliou

Abstract— Towards enabling bandwidth-hungry 5G applications, a Fiber-Wireless (FiWi) mobile fronthaul architecture is experimentally presented supporting the co-existence of spectrally efficient analog transport formats with Digital Radio over Fiber transport schemes, combined with millimeter wave (mmWave) high-capacity wireless channels. Flexible transport network reconfiguration is proposed by means of a low-loss 1×4 Si_3N_4 Reconfigurable Optical Add/Drop Multiplexer (ROADM) on TriPleX platform, selectively dropping four FiWi mmWave fronthaul links to four different antenna location. Detailed investigations of the proposed system are reported, including frequency characterization, multi-stage EVM penalty study and analog/digital traffic coexistence PHY layer feasibility. Following, four 10 Gb/s multi-band 16-QAM WDM FiWi analog IFoF links are transmitted through 10km fiber and 1-m directional V-band antennas and flexibly reconfigured by a Si_3N_4 ROADM, achieving a record 40 Gb/s wavelength-routed fronthaul capacity for mmWave 5G, while simultaneously meeting multiple 5G Use Cases within 3GPP requirements.

Index Terms—5G, C-RAN, Analog Radio-over-Fiber, Millimeter Wave, Fiber-Wireless, Reconfigurable Add/Drop Multiplexers.

I. Introduction

THE currently deployed 5th Generation (5G) of cellular networks has been designed not only towards enhancing the well-established 4th Generation (4G) in the short term, but rather to keep evolving towards meeting the requirements to unlock novel state-of-the-art applications such as Virtual Reality, Augmented Reality, Autonomous Vehicles, Internet-of-Things or Industrial Automation, which are now on the verge of massive commercialization [1]. As such novel technologies have been widely developed in the past years, they are expected to greatly benefit from the advent of a reliable, fully-flexible and high-capacity 5G infrastructure, designed to advance far beyond 4G in its functionalities.

Expert alliances have long defined precise 5G Key Performance Indicators (KPIs) [2], dictating connection capacities of up to 100 folds the typical user data rate, for tens of times more connected devices, resulting in 1000 times higher mobile data volume per geographical area [3], thus targeting figures such as 1 Gb/s/user and up to 10 Gb/s of peak aggregate traffic [4]. At the same time, a wealth of emerging bandwidth-hungry Use Cases has been laid out [5], such as Fixed-Wireless Access (FWA) and enhanced Mobile Broadband (eMBB) services, respectively unlocking ubiquitous 5G access in rural areas and providing high-capacity connectivity in the case of Hotspot scenarios as airports or stadiums, while still meeting the upper-mentioned KPIs. In turn, the implementation of these Use Cases is imposing significant challenges to the underlying infrastructure in terms of traffic capacity, whilst simultaneously poses the need to further evolve the network flexibility and reconfigurability, towards a completely agnostic approach on monitoring and controlling highly heterogeneous networks [6].

Thus, a fully Centralized Radio Access Network (C-RAN) architecture has been targeted by the 5G community, as envisioned to be capable to achieve multi-media, centralized network monitoring and control, while facilitating fast and cost-efficient deployment [7][8]. Additionally, C-RAN would provide the desired flexible network reconfigurability, by enabling the seamless integration and coexistence of heterogenous radio and optical access networks [9].

In this direction, along with the development of the underlaying optical transport network, upcoming 5G deployments are expected to gradually unlock commercial use of mmWave radio [10], to cope with the of extreme growth in cellular traffic [11]. With Global System for Mobile Communications (GSMA) supporting proper allocation of up to 800 MHz contiguous spectrum per operator in the mmWave [12], transforming the RAN section into a Fiber-Wireless (FiWi) network of unprecedented capacity [13].

As the previously mentioned multiplicity of applications have inherently different User-experience requirements, hence traffic demands, a multitude of optical-transport schemes with different spectral-efficiency characteristics would better fit to the variety of application-scenarios. Consequently, this implies a rising need to bring efficient Analog Radio over Fiber (A-RoF) for mmWave frequencies in co-existence with Digital-RoF (D-RoF).

Existing optical fronthaul infrastructure used to rely on bandwidth-consuming Common Public Radio Interface (CPRI) via D-RoF solutions, which raised serious concerns on the

This work is supported by H2020 5GPPP project Int5Gent (957403), 5G-PHOS (Contract No. 761989) and 5G STEP-FWD (Contract No. 722429). The authors would like to acknowledge Keysight for supporting the experiments with measurement equipment

E. Ruggeri, C. Vagionas, R. Maximidiss, G. Kalfas, D. Spasopoulos, N. Terzenidis, N. Pleros, A. Miliou are with the Department of Informatics, Center for Interdisciplinary Research and Innovation, Aristotle University of Thessaloniki, 54636 (e-mail: eugenior@csd.auth.gr).

Ruud M. Oldenbeuving, Paul W. L. van Dijk, Chris G.H. Roeloffzen are with LIONIX International B.V., Enschede, The Netherlands.

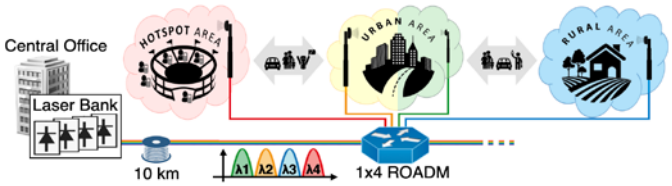

Fig. 1. Conceptual schematic of the proposed 5G fronthaul, providing flexible reconfiguration of the 4λ-WDM traffic between the Dense Urban, the Hotspot and the FWA Rural Areas.

spectral efficiency of the digital optical fronthaul [14][15]. Although requiring more complex RRHs, the enhanced CPRI (eCPRI) protocol has widely mitigated this situation by promoting higher layer functional splits, relaxing the insatiable data rate demand of the transport network by a significant 10-fold [16][17]. Nevertheless, as estimated by 3GPP [18], assuming a typical NR user bandwidth of 100 MHz and 32 antenna ports, the required transport bitrate would be of 9.8 Gbps in DL and 15.2 Gbps in UL [19]. Of course, the use of optical interfaces with high-order modulation format can be of support, nevertheless, with such high figures, an enhanced spectral efficiency would be greatly preferred, possibly supporting eCPRI in its limitations by complementing it while coexisting on the same physical infrastructure.

In this direction, A-RoF shows its stronghold in bandwidth efficiency, relying on native radio signals being modulated directly on the optical carrier, without requiring any extra bandwidth overhead [20][21], with demonstrations of up to 1Tb/s CPRI equivalent rate [22]. Moreover, as already employed in Metro Networks [23] and Passive Optical Networks (PONs) [24], Wavelength Division Multiplexing (WDM) techniques are well-established in providing one extra dimension in traffic parallelization [25], by inserting optical multiplexing devices at the antenna site and running over field-deployed single mode fibers [9], avoiding costly brownfield fiber installation. In this direction, WDM-enabled A-RoF schemes have additionally been demonstrated to support radio frequency channel aggregation of 12×211 MHz-bandwidth f-OFDM signals [26] and 4×2.5 Gb/s in a 60 GHz RoF experimental demonstration [27]. Gaining increased popularity as valid alternative to D-RoF, albeit dissimilar, A-RoF schemes could be introduced whether the need raises for spectral efficient transport beyond the eCPRI capabilities, e.g. on capacity-demanding deployments, in coexistence with the current digital network infrastructure [28].

At the same time, as ROADMs have shown to enable flexible network reconfigurability capabilities in metro-access networks [29][30], although relying on costly and bulky Wavelength Selective optical Switches (WSS) [31] or micro-electro-mechanical systems (MEMS) [32], several developments of similar, smaller scale ROADMs, with lower number of ports, have been proposed in the past as suitable solutions for the much stricter, cost-efficient Access Network segments [33]-[36]. These early stage mini-ROADM devices have demonstrated up to 40 Gb/s Non-Return-to-Zero-On-Off-Keying (NRZ-OOK), for a 4×4 Semiconductor Optical Amplifier-based photonic integrated Wavelength Division Multiplexing cross-connect [37], while supporting for up to 12×10-Gb/s CPRI channel×linerates [33], although inherently limited by the CPRI bandwidth overhead. In addition, stemming from recent advances in CMOS technology and Silicon Photonics (SiPho), novel mini-ROADMs have been recently presented, characterized by low-loss, wide-bandwidth and high-level of miniaturization [33][38], showing great potential for further reducing fabrication costs and thus opening a path towards plausible 5G Access Network implementation. Additionally, as FiWi A-RoF/IFoF links have recently started to unravel immense aggregate traffic capacity of up to 219 Gb/s [39], similar integrated photonic packaged OADMs with fiber-to-fiber losses in the range of 10 dB [40] or polarization insensitive operation [41] are currently being developed, which would eventually relieve potential in-field implementations from the use of automatic polarization controllers.

While low-loss, cost-effective, small scale, integrated photonic ROADMs have been proposed in the literature towards enabling flexible reconfiguration capabilities in high-capacity C-RAN architectures [34][35], current reconfigurable fronthaul demonstrations have been limited either in A-RoF/IFoF mmWave links only, being limited to 7.5Gb/s/λ often with wired EDFA-assisted setups [34] or in D-RoF fronthaul networks [33][35], without showing co-existence of multiple A-RoF/IFoF and D-RoF fronthaul formats.

In this work, the authors aim to show co-existence and arbitrary reconfiguration of 10 Gb/s analog or digital data streams through an optically unamplified, low-loss, integrated photonic 1x4 Si_3N_4 ROADM towards different geographical radio sites, as envisioned by the concept of Fig. 1, providing flexible high-capacity connectivity to Urban, Rural and Hotspot areas, following the needs of a typical wide cellular network. Extending our previous 4λ×1 Gb/s FiWi beamsteering links [35] and 40 Gb/s FiWi record capacity demonstration [13], we present a more detailed experimental demonstration of four parallel 10 Gb/s WDM IFoF/V-Band FiWi fronthaul architecture across a 10 km fiber and 50 cm of V-band distance, arbitrarily reconfigured by a low-loss Si3N4 ROADM. Additionally, experimental demonstrations of ubiquitous re-routing of the same optical carrier towards four radio sites and of analog/digital coexistence on the same physical layer are presented. In full 4λ-WDM configuration, each of the four reconfigurable FiWi mmWave links transports four IFoF 625-Mbaud 16-QAM data streams for an aggregate of 16 IFoF channels with EVM quality that meets the 3GPP metrics [42]. To the authors' knowledge, the current work forms the record reconfigurable capacity for FiWi mmWave networks, while supporting optically unamplified ROADM operation with A-RoF/IFoF and D-RoF co-existence.

II. Experimental Setup and Devices

The experimental setup of the proposed reconfigurable multi-λ and multi-band fronthaul system, as presented by the authors in [13], is shown in Fig. 2(a), including dedicated labels for each of the three distinct sections, represented with different background colors. The first two sections are purely of optical nature, being respectively an IFoF optical transmission section, depicted in Fig. 2(a) with light-yellow background, and an IFoF optical propagation and routing section, in light red-background. The third and last section includes the opto-electric conversion along with a 1-m PtP V-Band directional wireless link [13], this time in light-blue background. While this work focuses on the downlink direction, a symmetrical uplink configuration could be feasible based on [43].

Ref	Date	#Ch.	OTA	w/o Opt. Ampl.	IL (dB)	Data Rate
[X]	2016	12	x	x	12	120 Gb/s
[X]	2016	8	x	x	15	0.8 Tb/s
[X]	2017	4	x	x	6	40 Gb/s
[X]	2020	10	x	x	10-15	7.5 Gb/s
[X]	2010	8	✓	x	-	1.24 Gb/s
[X]	2015	9	✓	x	5.5	13.5 Gb/s
[X]	2021	4	✓	✓	5	4 Gb/s
This work	2022	4	✓	✓	5	40 Gb/s

Table 1 – State of the art for reconfigurable Fiber-Wireless demonstrations. From left to right: reference, date, number of used channels, if over-the-air is performed, if optical amplification is employed, insertion loss, data rate.

At the IFoF optical transmission stage of the setup, from left to right, the optical transmission section features four Continuous Wavelengths (CWs), generated by a 4-channel Tunable Laser Source (TLS) and centered around 1550nm, with DWDM-compliant spacing of 0.8nm, namely λ_1=1547.38 nm, λ_2=1549.78 nm, λ_3=1549.06 nm and λ_4=1548.22 nm. The four optical carriers are then merged into DWDM traffic by a 4×1 coupler, before being fed to a 10 GHz Mach Zehnder Modulator (MZM), while separately optimizing the respective polarization states by means of four manual Polarization Controllers (PC). An electrical waveform featuring four 64-QAM 625 MBaud bands, synthetized and digitally upscaled around 2.5 GHz IF by an Arbitrary Waveform Generator (AWG), is first amplified to about 5 V and then imprinted on all four optical carriers via the MZM, biased at 3.2 V for enhanced linearity of operation. For an in-field deployment, the traffic carried by the pure physical layer is to be shared between user and management planes.

At the optical propagation and routing section of the setup, the generated DWDM IFoF traffic enters the propagation and routing section, with a 10 km of SMF, emulating a typical mobile fronthaul (MFH) network with α=0.2 dB/km, before passing through the last PC and the polarization dependent low-loss ROADM device for physical optical reconfiguration.

The employed ROADM by Lionix is realized by a lattice of cascaded MZI-interleavers, exhibiting 0.8 nm of spacing, 32.5 GHz flat-top passband and below 0.02 dB power variation between the upper/lower sideband [35]. In order to achieve the desired reconfigurable demultiplexing operation, the MZI based building blocks rely on electronically-tunable optical couplers, which are in turn guaranteeing flat-top response and compensation for any undesired non-ideal filter transfer function caused by the fabrication process. Integrated on an ultra-low loss Si_3N_4/SiO_2 TriPleX platform [46], the ROADM device is characterized by only 5 dB of fiber-to-fiber losses in average, while providing the transfer function displayed in Fig. 2(c). Electronically controlled in temperature, the employed ROADM prototype is experimentally investigated to have negligible EVM penalty for crosstalk values below -15 dB for 16-QAM modulation format [47]. As displayed in a color-coded manner, Fig. 2(c) describes how each pass-band ROADM's output is finely tuned for each corresponding incoming wavelength, with $\lambda_{1\text{-}4}$ simultaneously exiting the device from different, selected ports. In Section V an extensive discussion of the several possible configurations that allows for fully reconfigurable demultiplexing operation, is presented (Fig. 2(c) represents one of these). The ROADM device also represents the last optical component of the proposed IFoF optical propagation and routing section which, in total, exhibits average end-to-end optical insertion losses as low as 7 dB.

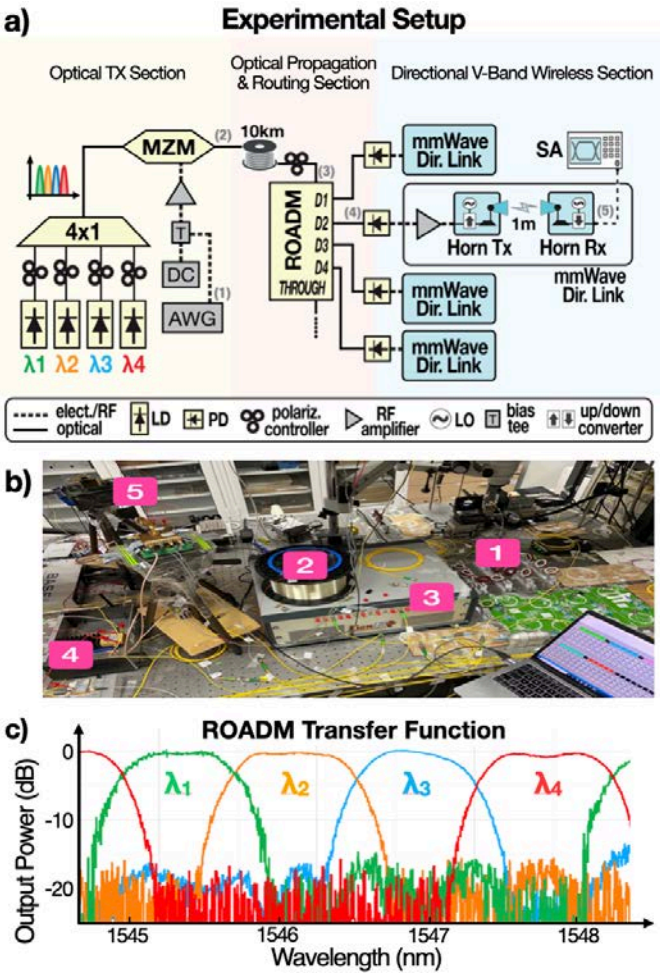

Fig. 2. Experimental setup of the proposed fully analog system, highlighting the three colored sections and displaying the five stages of the signal propagation in light grey numbering, i.e., from (1) to (5). The optical components are represented with yellow blocks, while the wireless with blue ones. b) Labelled photo of exp setup: 1) 4x optical sources 2) 10 km spool 3) ROADM 4) RF amplifier 5) mmWave channel. c) The optimized ROADM transfer function employed for both of the full 4λ-WDM traffic demonstr.

Following the optical propagation and routing section, each of the 4 outputs of the ROADM device is then driven to the V-Band wireless section of the setup, thus entering a 10 GHz PIN Photoreceiver (PD) for opto-electrical conversion, which recovers the initial four 64-QAM RF-bands of 625-MBaud to be forwarded to the V-Band wireless channel. The upper-mentioned electrical waveform is amplified to around +7 dBm before being fed to a V-Band horn antenna Tx assembly, featuring a 22.5-dBi directional horn antenna element, power amplifier, mixer and a ×6 multiplier used to generate the 60 GHz radio carrier, by means of a 10 GHz reference signal produced by an external Local Oscillator (LO). Downstream, a 1-m Over-The-Air (OTA) V-Band wireless propagation is employed, selected due to spacing and cabling limitations of the laboratory environment [13][48]. Following, the mmWave OTA 60 GHz signal is then captured by a symmetrical V-Band horn antenna Rx assembly and driven to a Signal Analyzer (SA) for evaluation purposes in terms of EVM figure.

III. Frequency Response and Wireless Bottleneck

Targeting to stress the proposed fronthaul system in terms of highest possible capacity, the authors have performed two separate frequency response evaluations, first on the optical-

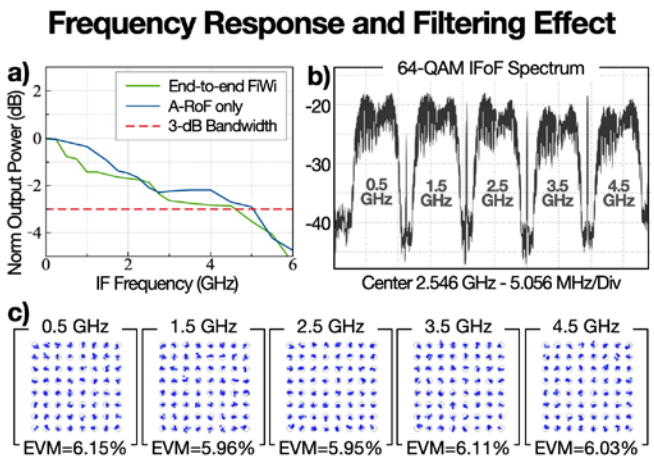

Fig. 3. a) Frequency responses of the IFoF optical-only and of the end-to-end FiWi links, featuring 4.5 GHz and 5 GHz of 3-dB bandwidth, respectively. b) Spectrum and correspondent c) constellation diagrams of the IFoF 64-QAM analog transmission.

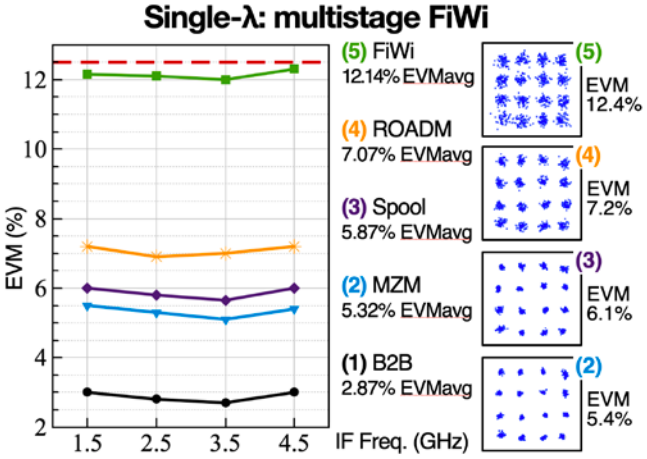

Fig. 4. Experimental results of the multi-stage investigation of the end-to-end single-λ FiWi link, plotting EVM figure of each of the four bands with the respective average performance, along with constellation diagrams of the 4th band for each significant stage of the system.

only IFoF sections, up to 10 GHz PIN PD, and then on the full end-to-end IFoF/V-Band FiWi path, thus also including the directional V-Band wireless link contribution of the third, electrical section. For these two case studies, as for the rest of Section III and IV, the ROADM device is to be considered configured for multi-λ 1×4 channel operation, as depicted in Fig. 2(c), while specifically using only the pass-band channel of λ_2, identified as the worse performing, towards investigating the maximum single-λ capacity of the proposed system.

Starting from the optical IFoF path, the frequency response revealed a 3-dB bandwidth of 5 GHz, as depicted in Fig 3(a). It is worth noting that, the ROADM prototyped device was designed and tested for supporting over 30 GHz of flat-top passband and was not found to impose any additional bandwidth limitation. On the other hand, for the case of the end-to-end FiWi propagation, the frequency response based on a single-tone sweep presented in [13] and reported in in Fig. 3(a) of this extension, shows a measurement of 3-dB bandwidth of 4.5 GHz. The differential 500 MHz of filtering effect is to be attributed to the RF gain chain of the wireless section, which allows for higher power density but at the expense of a portion of bandwidth range.

Following the frequency response evaluation, the same two configurations, represented by the optical subsystem and the end-to-end link configurations, were additionally tested in terms of maximum data transmission. Extending our previous work [13], 5×3.750-Gb/s bands were successfully transmitted by the optical-only subsystem, each carrying 625 MBaud of 64-QAM, for a total aggregate capacity of 18.750 Gb/s/λ. The resulting RF spectrum and constellation diagrams, after opto-electrical conversion of the IFoF signal, are reported in Fig 3(b) and 3(c) respectively, achieving a 6.04% average EVM well-below the 8% threshold defined by 3GPP for 64-QAM modulation format [40].

On the other hand, the motivation towards further enhancing the optical sections comes up short, as the same principle does not apply for the case study of the full end-to-end configuration presented in [13], featuring the challenging V-Band wireless section which requires high gain values due to the lossy mmWave OTA transmission. In fact, as the filtering effect discussed in [13] allows for successful transmission of only 4×625-MBaud 16-QAM bands through the end-to-end system, achieving a total aggregate Fiber-Wireless capacity of 10 Gb/s/λ, the electrical noise stemming from the several high-power RF components prevents from achieving higher SNR values for all four bands simultaneously, thus imposing a limit on the chosen modulation format. Nevertheless, following this rationale, it is possible to claim that the Fiber-Wireless capacity of the system could be further extended by optimizing the design and operation of the third, wireless section only, as previously discussed by the authors in [48].

IV. Single-λ Multi-Stage Degradation Study

Stemming from the previous considerations about the few electrical and optical bottlenecks identified along the complex Fiber-Wireless proposed system, a thorough performance-degradation study across the various stages of the set-up was performed for one of the four FiWi transmissions, corresponding to λ_2 as discussed in Section III, while carrying the 4×625-MBaud 16-QAM 10 Gb/s traffic.

The plots reported in Fig. 4 [13] describe the EVM figures of each of the four RF bands at each of the five stages, identified by the numbering inserted in the experimental setup of Fig 2(a). Additionally, Fig. 4 reports for each stage, the constellation diagram corresponding to the 4th band, which was identified as the worse performing RF channel, showing some saturation due to the high amount of injected power necessary to compensate the inherently higher attenuation of the higher band. Starting from the electrical back-to-back measurement and following the signal propagation through each stage of the proposed system, the first consistent degradation is attributed to the RF amplification prior to the electro-optical conversion, showing a significant 2.45% EVM penalty between the unamplified back-to-back electrical waveform and the optical output of the MZM (points (1) & (2)). On the other hand, the optical propagation through the 10 km spool and the ROADM operation together are imposing a 1.75% EVM degradation (points (2) & (4)), with the demultiplexing operation alone, performed by the ROADM prototype device, having a relatively small impact of just 1.2% EVM penalty (points (3) & (4)). Exiting the IFoF optical propagation and routing section, the multi-band waveform sustains the highest impact of over-5% degradation in EVM

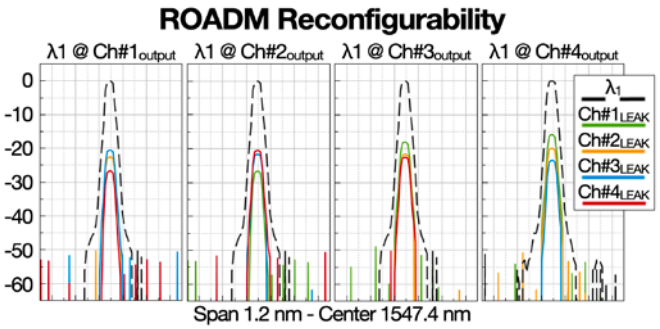

Fig. 5. Optical spectra corresponding to the four ROADM output channels, from Ch#1 to Ch#4, from left to right, providing proof-of-principle of ubiquitous re-routing of λ_1 to any selected output channel.

performance (points (4) & (5)) by the challenging V-Band wireless section, due to the previously discussed high gain required to compensate the lossy V-Band channel [48][49].

Moreover, a Noise Figure of at least 10.5 dB was estimated by comparing the initial SNR with the system's output, while 17.5 dB of Spurious Free Dynamic Range (SFDR) were calculated stemming from the comparison between the measured in-band and out-of-band peak powers. In any case, after taking in consideration all the imposed degrading contributions, the proposed IFoF/V-Band FiWi system still performs within the 12.5% EVM threshold defined by 3GPP [40], for all cases.

V. ROADM Ubiquitous λ Reconfiguration Proof-of-Principle

Since the focus of this work is to demonstrate multi-λ maximum aggregate traffic capacity through the proposed system, while arbitrarily delivering multiple 10 Gb/s streams towards different cell-sites and antenna-locations, a proof of principle of ubiquitous reallocation of one optical carrier to any of its four possible output Drop ports is presented in the following. For the sake of this investigation, the authors have experimentally found four possible ROADM configurations, towards demonstrating its inherent capability to re-route each λ towards any arbitrary output of the device, by simply employing different transfer function configurations, finely controlling the electronically-tunable optical couplers of the ROADM. Specifically, this proof-of-principle experimental demonstration features ubiquitous re-routing of λ_1 towards each of the four available outputs. This is performed, for each re-route of λ_1, with the three remaining optical carriers being tuned to operate normally on the 3 remaining ROADM channels respectively, to monitor their correspondent optical power leakages on λ_1's channel. For instance, in the first case of Fig 5, i.e. "λ1 at CH#1 output", λ1 is injected into CH#1 input and captured at CH#1's output, while λ_2, λ_3 and λ_4 are respectively injected into CH#2, CH#3 and CH#4 their power leakage on CH#1 is measured.

Fig. 5 reports the spectra of the four cases, from left to right, of re-routing λ1 to the ROADM output channels #1 to #4, while also showing the leaked optical power coming from the remaining analog traffic. As described by the legend of Fig. 5, λ_1 is displayed with a dashed black line for all four cases, while the remaining optical carries are displayed following the previously defined color code of Fig. 2(c). These four spectra show more than 15 dB of difference between spectral peaks of

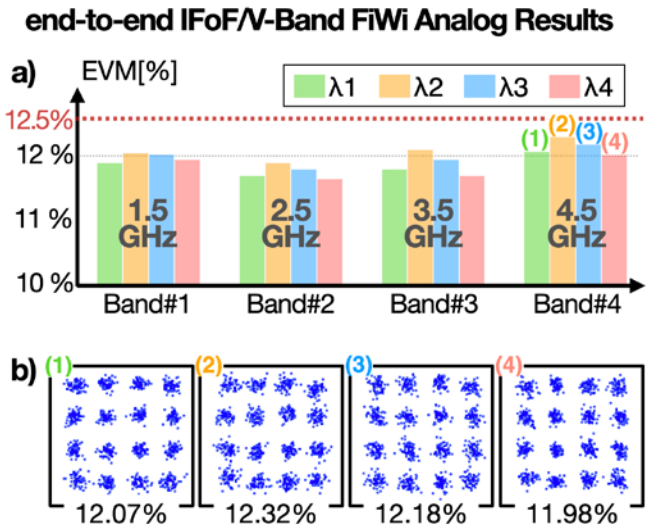

Fig. 6. a) Histogram of the multi-band multi-λ demonstration, reporting the EVM figure of each band after end-to-end IFoF/V-Band transmission, displayed by color-coded λ. b) The four constellation diagrams corresponding to the worst-case scenario of the 4th band, respectively from λ_1 to λ_4.

the desired λ_1 at each output channel and the other three optical carriers, proving negligible crosstalk to λ_1. This proves, in turn, that any optical carrier could be arbitrarily re-routed towards any of the ROADM outputs, given the proper configuration of the ROADM prototype, which could be remotely programmed by the controller of a network operator in a realistic fronthaul network scenario.

VI. Record 40 Gb/s Analog Traffic Capacity & D-RoF Coexistence

Following the thorough characterization of the proposed system, the full 4λ-WDM traffic is experimentally evaluated towards demonstrating flexible allocation of the parallel 10 Gb/s fronthaul streams towards different physical locations, i.e. antenna sites, toward meeting 5G eMBB Hotspot targeted capacities [50]. Specifically, the four parallel analog streams are routed towards four end-point antenna locations that could in-principle be scattered at a second local urban dense scenario, a high-capacity demanding hotspot or a rural FWA scenario. Additionally, one of the four analog wavelengths is then replaced by a D-RoF stream, showing feasible coexistence of the two transport schemes on the same physical network, with no further tuning or optimization.

A. 4λ-WDM 40-Gb/s Record Aggregate Analog Traffic

Towards loading the maximum possible capacity on the presented Fiber-Wireless infrastructure, the full 4λ-WDM traffic is launched into the system, with each λ respectively carrying four 2.5-Gb/s RF bands and the ROADM device being configured for full traffic demultiplexing operation, thus enabling all four outputs as described in Section II.B and depicted in Fig. 2(c). Given these parameters, each of the four wavelengths, carrying the 4×625-MBaud 16-QAM 10 Gb/s traffic, is then routed to each of the four outputs of the ROADM before being successively fed to the directional V-Band wireless section for OTA transmission.

The histograms of Fig 6(a) are representative of the electrical signal quality exiting the V-Band wireless section, as captured by the SA with no additional customized digital signal

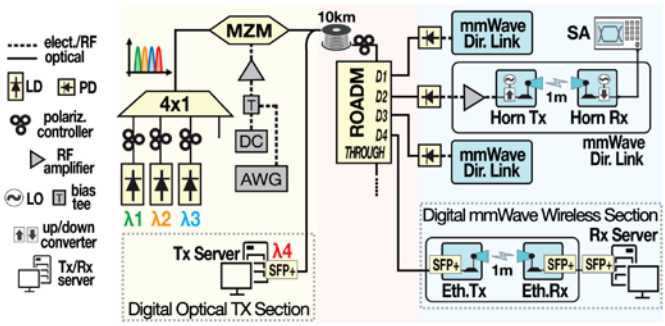

Fig. 7. Experimental setup of the proposed analog-digital coexistence system, highlighting the three colored sections and displaying the newly introduced digital optical transmission and digital V-Band wireless sections. The optical components are represented with yellow blocks, the wireless with blue ones.

processing (DSP). As briefly presented by the authors in [13], Fig 6(a) depicts the EVM value obtained by each RF band of each corresponding λ exiting the proposed Fiber-Wireless system, while Fig 6(b) reports the four constellation diagrams corresponding to the worse performing RF band, i.e. the 4th, showing clearly demodulated points. With the slight increase in EVM penalty for the 4th band to be attributed mainly to the bandwidth penalty imposed by the wireless section filtering effect. Meeting in all cases the 12.5% 3GPP threshold for 16-QAM [40], while satisfying the 1 Gb/s and 10 Gb/s KPIs defined by Next Generation Mobile Network Alliance (NGMNA) for single user channel and aggregate peak traffic performance [4], respectively, this experimental demonstration proves a record total aggregate analog capacity of 40 Gb/s.

B. Seamless Analog and Digital RoF Coexistence

While maintaining the same exact operational settings described for the 40 Gb/s analog transmission, the authors have performed a coexistence evaluation with a digital stream of D-RoF data, when keeping the remaining analog traffic running at all times.

One of the four optical analog streams, i.e. λ_4, was replaced by an industry-compliant server-based transmission employing a 10-Gb/s SFP+ D-RoF transceiver of consistent optical wavelength, as depicted in the experimental setup of Fig. 7, forming a standalone digital optical transmission section, before entering the common optical propagation and routing section of the system in parallel with the analog stream. As for the three analog channels already in place exiting the ROADM device, also the D-RoF stream is injected in the ROADM input by means of an optical coupler, demultiplexed and forwarded to the respective 5-Gb/s mmWave digital antennas section.

Following, a pair of directive digital mmWave commercial antennas take place on the wireless link of the digital stream, characterized by 5 Gb/s of OTA traffic capacity and (SFP+)-enabled input/output, thus not requiring the use of an external PD and forming a standalone digital mmWave wireless section. As depicted in Fig. 7, the digital wireless transmitter takes as input the 10 Gb/s digital traffic exiting the common optical propagation and routing section by means of an SFP+ transceiver, which performs the opto-electrical conversion providing electrical ethernet traffic directly to the digital wireless transmitter. Vice-versa, after the 5 Gb/s mmWave OTA transmission, the digital wireless receiver employs an

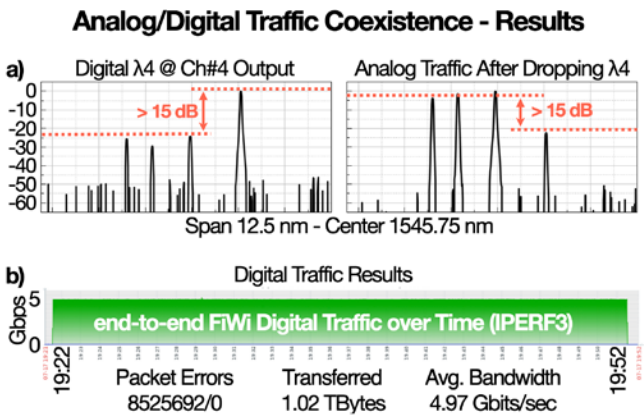

Fig. 8. a) Spectrum of the ROADM output at Ch#4, featuring the demultiplexed digital λ_4, on the left-hand side, and the remaining three analog carriers, after dropping λ_4, on the right-hand side. b) IPERF3 results of the digital end-to-end FiWi stream captured and evaluated by the Rx server.

identical SFP+ optical transceiver to capture the received electrical ethernet traffic and optically drive it towards the receiving server for evaluation of the stream performance.

As depicted on the right-hand side of Fig. 8(a), the optical traffic exiting the ROADM from Ch#4 shows proper demultiplexing of the digital λ_4, while the left-hand spectrum of Fig 8(a) depicts the part of the 4λ-WDM traffic featuring the remaining three analog optical carriers. Respecting the 15 dB of differential peak power in favor of the desired optical signals in both cases, thus maintaining the necessary performance to allow proper demodulation, as discussed in [47], the coexistence of analog and digital optical traffic is shown to have negligible effect on the optical path.

Then, following the OTA transfer of the digital traffic, the digital stream performance is evaluated, over a timeslot of 30 consecutive minutes, by a server-based IPERF measurement in terms of physical layer parameters such as transferred capacity and average bitrate. With a total transferred capacity of 1 TByte over 30 minutes of almost-flat 5 Gb/s operation, as depicted in Fig 8(b), a successful transmission of a total 35 Gb/s heterogenous aggregate traffic was seamlessly demonstrated on the proposed system, requiring no further tuning or adjustment of any optical or RF component, while the remaining analog traffic was monitored to maintain the same performance described in Section VI.A at all times.

VII. Conclusions

An experimental demonstration of optically unamplified IFoF/V-Band FiWi transmission through a 100GHz Si_3N_4 ROADM was presented, featuring 4.5 GHz of end-to-end 3-dB bandwidth. One 64-QAM optical multi-band data stream was initially transmitted through a wired-only setup, before a thorough end-to-end investigation of a 4×625-MBaud 16-QAM signal flow, carried out in terms of EVM metric, by capturing the waveform at several specific points-of-interest of the proposed system.

While the single-λ multi-stage evaluation revealed the highest EMV degradation, of above-5%, to be attributed to the V-Band mmWave OTA transmission, the ROADM capability to properly manage ubiquitous reconfiguration of four of such 10 Gb/s traffic streams was experimentally endorsed by a successful proof-of-principle.

Following, the full traffic comprising of four optical carriers, each one carrying the 10-Gb/s 4×625-MBaud 16-QAM data streams, was loaded on the IFoF/V-Band FiWi system. With a record aggregate capacity of 40 Gb/s within the 3GPP-defined requirements, this demonstration extends our previous work [13], while satisfying multiple 5G Use Cases over the same network architecture. Moreover, by simply replacing one analog carrier with an SFP-based 5 GB/s digital FiWi stream, this work additionally aims to support feasibility of analog/digital traffic coexistence on the same system architecture, with an heterogeneous aggregate data rate of up to 35 Gb/s, while meeting the 3GPP requirements in all cases.

REFERENCES

[1] Ó. Blanco-Novoa et al., "A Practical Evaluation of Commercial Industrial Augmented Reality Systems in an Industry 4.0 Shipyard," in IEEE Access, vol. 6, pp. 8201-8218, 2018.

[2] Next Generation Mobile Networks Alliance, “5G White Paper,” 2015. [Online]

[3] 5GPPP, “Key Performance Indicators”. [Online]

[4] Next Generation Mobile Networks Alliance, “NGMN 5G White Paper,” Feb. 2019.

[5] G. Brown, "Exploring 5G New Radio: Use Cases, Capabilities & Timeline," Qualcomm White Paper, Sept. 2016.

[6] N. Slamnik-Kriještorac et al., "Sharing Distributed and Heterogeneous Resources toward End-to-End 5G Networks: A Comprehensive Survey and a Taxonomy," in IEEE Communications Surveys & Tutorials, vol. 22, no. 3, pp. 1592-1628, thirdquarter 2020.

[7] C. Ranaweera et al., "5G C-RAN architecture: A comparison of multiple optical fronthaul networks," 2017 International Conference on Optical Network Design and Modeling (ONDM), pp. 1-6, 2017.

[8] Jun-ichi Kani, Jun Terada, Ken-Ichi Suzuki, and Akihiro Otaka "Solutions for future mobile fronthaul and access-network convergence," J. Lightwave Technol., 35 (3), 527-534, 2017.

[9] G. Kalfas et al., "Next Generation Fiber-Wireless Fronthaul for 5G mmWave Networks", IEEE Com. Mag., 57 (3), 138, March 2019.

[10] Verizon, Press Release, “Fastest 5G Network in the World just got bigger and better”, 13 Oct. 2020 Article in Press. [Online]

[11] B. Schrenk et al., "Fully-Passive Optical Switch Introducing Dynamicity and Flexibility to Metro-Access," IEEE PTL, 27 (5), 486, 2015.

[12] “5G Spectrum GSMA Public Policy Position”. [Online]

[13] E. Ruggeri et al., “4×10 Gb/s WDM Fiber Wireless multi-IFoF Reconfigurable Fronthaul using a low-loss Si3N4 ROADM for mmWave 5G”, in 2021 Optical Fiber Comm Conf and Exhibit (OFC), pp. 1-3, 2021.

[14] M. Rebato et al., "Multi-Sector and Multi-Panel Performance in 5G mmWave Cellular Networks," in IEEE Global Communications Conference (GLOBECOM), Abu Dhabi, United Arab Emirates, 2018.

[15] Pham Tien Dat et al., "5G transport networks: the need for new technologies and standards," IEEE Comm Magazine, 54, (9), 18-26, 2016.

[16] H. Yu, et. al. "100Gbps CWDM4 Silicon Photonics Transmitter for 5G applications," OFC, W3E.4, San Diego, CA., USA, March 2019.

[17] Ericsson AB, Huawei Technologies Co. Ltd, NEC Corporation and Nokia, “Common Public Radio Interface: eCPRI presentation”. [Online]

[18] 3GPP TR 38.801 V14.0.0, “3rd Generation Partnership Project; Technical Specification Group Radio Access Network; Study on new radio access technology; Radio access architecture and interfaces”, Release 14, 2017.

[19] 5G Fundamentals: Functional Split Overview. [Online]

[20] C. Lim et al., "Evolution of Radio-over- Fiber technology", J. Lightwave Technol., 37 (6), 1647-1656, 2019.

[21] P. T. Dat et al., "Radio-on-radio-over-fiber: efficient fronthauling for small cells and moving cells," IEEE Wirel. Comm., 22 (5), 67, 2015.

[22] Shota Ishimura et al., “1.032-Tb/s CPRI-equivalent rate IF-over-fiber transmission using a parallel IM/PM transmitter for high-capacity mobile fronthaul links”, J. Lightwave Technol., 36(8), 1478-1484, 2018.

[23] E. Ruggeri et al, "Fiber Wireless A-RoF/IFoF uplink of 0.4Gb/s 16-QAM and 0.6Gb/s QPSK over a 32-element 60GHz phased array antenna for 5G fronthaul networks," IEEE MWP, Ottawa, Canada, Oct. 2019.

[24] U. Habib et al., "Single Radio-Over-Fiber Link and RF Chain-Based 60 GHz Multi-Beam Transmission," in Journal of Lightwave Technol., vol. 37, no. 9, pp. 1974-1980, May 2019.

[25] M. Sung et al., "Demonstration of IFoF-Based Mobile Fronthaul in 5G Prototype With 28-GHz Millimeter wave," in Journal of Lightwave Technology, vol. 36, no. 2, pp. 601-609, Jan. 2018

[26] Y. Zhu et al., "Experimental Demonstration of a WDM-RoF Based Mobile Fronthaul With f-OFDM Signals by Using Directly Modulated 3s-DBR Laser," in Journal of Lightwave Technology, vol. 37, no. 16, pp. 3875-3881, 15 Aug.15, 2019.

[27] Z. Cao et al., "WDM-RoF-PON Architecture for Flexible Wireless and Wire-Line Layout," in IEEE/OSA Journal of Optical Communications and Networking, vol. 2, no. 2, pp. 117-121, February 2010.

[28] Z. Zakrzewski et al., “D-RoF and A-RoF Interfaces in an All Optical Fronthaul for 5G Mobile System”, in Applied Sciences, February 2020.

[29] P. Iovanna, et. al. “A Future Proof Optical Network Infrastructure for 5G Transport”, JOCN, 8 (12), 2016.

[30] S.Nakamura, "Optical Switches Based on Silicon Photonics for ROADM Application," IEEE JSTQE, 22 (6), 2016.

[31] S. J. Fabbri, S. Sygletos, A. Perentos, E. Pincemin, K. Sugden, and A. D. Ellis, “Experimental implementation of an alloptical interferometric drop, add, and extract multiplexer for superchannels,” J. Lightwave Technol., vol. 33, no. 7, pp. 1351–1357, 2015.

[32] K. Yamaguchi, Y. Ikuma, M. Nakajima, K. Suzuki, M. Itoh, and T. Hashimoto, “M×N wavelength selective switches using beam splitting by space light modulators,” IEEE Photon. J., vol. 8, no. 1, 0600809, 2016.

[33] V. Sorianello, “Polarization insensitive silicon photonic roadm with selectable communication direction for radio access networks” Opt. Lett., vol. 41, no. 24, pp. 5688–5691, Dec. 2016.

[34] C. Browning, "A Silicon Photonic Switching Platform for Flexible Converged Centralized-Radio Access Networking," JLT, 38 (19), 2020.

[35] A. Tsakyridis et al., "Reconfigurable Fiber Wireless IFoF Fronthaul With 60 GHz Phased Array Antenna and Silicon Photonic ROADM for 5G mmWave C-RANs," in IEEE Journal on Selected Areas in Communications, vol. 39, no. 9, pp. 2816-2826, Sept. 2021.

[36] C. Mitsolidou et al., "A 5G C-RAN Architecture for Hot-Spots: OFDM based Analog IFoF PHY and MAC Layer Design", EuCNC, 2019.

[37] Calabretta, N.; Miao, W.; Mekonnen, K.; Prifti, K. SOA Based Photonic Integrated WDM Cross-Connects for Optical Metro-Access Networks. Appl. Sci. 2017, 7, 865.

[38] C. R. Doerr, “Silicon photonic integration in telecommunications”, frontiers in Physics, vol. 3 article 37, (2015).

[39] S. Ishimura, "Multi-IF-over-fiber transmission using a commercial TOSA for analog fronthaul networks aiming beyond 5G," OpEx, 2021.

[40] S. Lee et al., "Consolidation of a Metro Network into an Access Network based on Long-reach DWDM-PON," in Optical Fiber Communication Conference and Exposition and The National Fiber Optic Engineers Conference, Technical Digest, paper NWA2, 2006.

[41] Klinkowski, M. et al., “Planning of Optical Connections in 5G Packet-Optical xHaul Access Network” Appl. Sci., 12, 1146, 2022.

[42] 3GPP TS38.104, "5G; NR; Base Station (BS) radio transmission and reception", v.15.2.0, 2018-7.

[43] K. Atra et al., "An InP Reflective SOA-EAM for 10 Gb/s Colorless Multi-IFoF/mmWave Fiber-Wireless Uplink in 5G Networks," in CLEO, paper SW3A.6, 2021.

[44] T. Kuri et al., "Reconfigurable Dense Wavelength-Division-Multiplexing Millimeter-Waveband Radio-Over-Fiber Access System Technologies," in Journal of Lightwave Technology, vol. 28, no. 16, pp. 2247-2257, Aug.15, 2010.

[45] B. Schrenk, et al., ”Towards spectrum-programmable, mesh-enabled mobile xHaul through reconfigurable WDM overlay in fully-passive networks," 17th International Conference on Transparent Optical Networks (ICTON), pp. 1-4, 2015.

[46] C. Roeloffzen et al., "Low-Loss Si3N4 TriPleX Optical Waveguides: Technology and Applications Overview", IEEE JSTQE, 24(4), 2018.

[47] E. Ruggeri et al., "A 5G Fiber Wireless 4Gb/s WDM Fronthaul for Flexible 360° Coverage in V-Band massive MIMO Small Cells," in Journal of Lightwave Technology, vol. 39, no. 4, pp. 1081-1088, 15 Feb.15, 2021.

[48] C. Vagionas et al., "Linearity Measurements on a 5G mmWave Fiber Wireless IFoF Fronthaul Link With Analog RF Beamforming and 120° Degrees Steering," in IEEE Communications Letters, vol. 24, no. 12, pp. 2839-2843, Dec. 2020, doi: 10.1109/LCOMM.2020.3019733.

[49] ETSI White Paper No. 9, “E-Band and V-Band - Survey on status of worldwide regulation”, first edition, June 2015, ISBN No. 979-10- 92620-06-1. [Online]

[50] Euro-5G (Supporting the European 5G Initiative) “D2.6 Final report on programme progress and KPIs” [Online]

View publication stats